Unidirectional molecular motor on a gold surface

van Delden, RA; ter Wiel, MKJ; Pollard, MM; Vicario, J; Koumura, N; Feringa, BL; Delden, Richard A. van

Published in:
Nature

DOI:
10.1038/nature04127

Supplementary Information

Unidirectional molecular motor on a gold surface

Richard A. van Delden, Matthijs K.J. ter Wiel, Michael M. Pollard, Javier Vicario, Nagatoshi Koumura, Ben L. Feringa*

Department of Organic Chemistry, Stratingh Institute, University of Groningen, Nijenborgh 4, 9747 AG Groningen, The Netherlands.

Section 1: Structural and photophysical characterization of **1** and **1-Au.**

Section 2: Structural and photophysical characterization of **2**.

Section 3: Experiments with *cis*-**3** to confirm the unidirectionality of rotary motion of **2** in solution.

Section 4: Experiments with *cis*-**4-Au** to confirm the unidirectionality of rotary motion on gold.

Section 5: General remarks

Section 1: *This section describes the characterization of molecular motors on gold nanoparticles.*

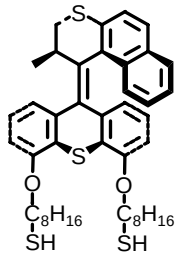

4,5-Bis[(8-sulfanyloctyl)oxy]-9-(2',3'-dihydro-2'-methyl-1'*H*-naphtho[2,1-b]thiopyran-1'-ylidene)-9*H*-thioxanthene (1)

^{1}H NMR (300 MHz, $CDCl_3$) δ 0.74 (d, *J* = 7.0 Hz, 3H), 1.20-1.65 (m, 20H), 1.87-2.00 (m, 4H), 2.50-2.58 (m, 4H), 3.08 (dd, *J* = 11.4, 2.6 Hz, 1H), 3.72 (dd, *J* = 11.4, 7.3 Hz, 1H), 3.90-4.20 (m, 5H), 6.02 (dd, *J* = 7.7, 1.1 Hz, 1H), 6.26-6.36 (m, 2H), 6.83 (d, *J* = 7.7 Hz, 1H), 6.99 (m, 1H), 7.09 (m, 1H), 7.20 (d, *J* = 7.5 Hz, 1H), 7.29 (m, 1H), 7.34 (d, *J* = 8.4 Hz, 1H), 7.53 (m, 3H).

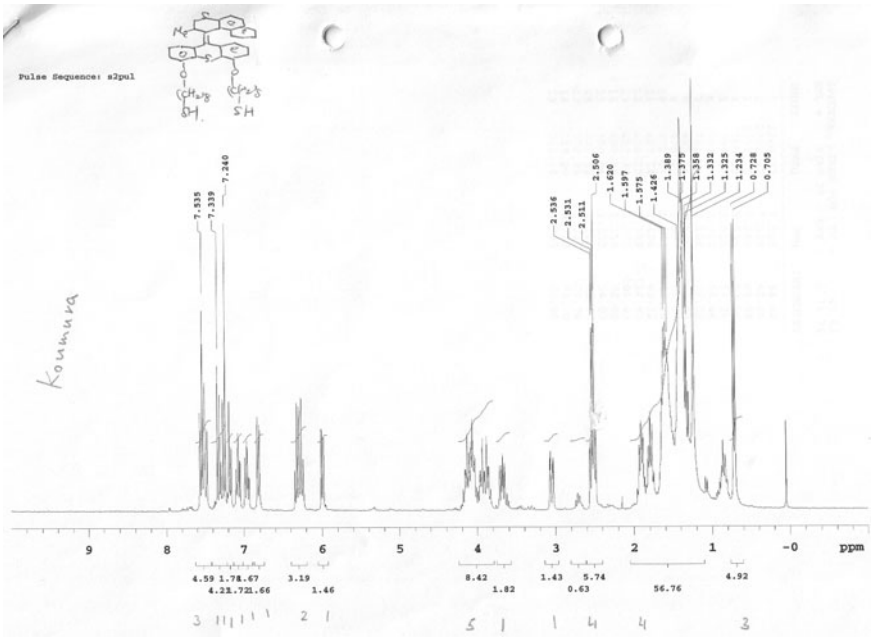

Figure 1: 400 MHz ^{1}H NMR of 1.

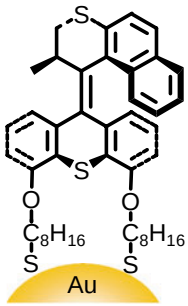

(2'*R*)-(*M*)-**1-Au**: Me_{ax}

Motor protected gold colloids 1-Au

To a mixture of Oct_4NBr (13 mg, 24 µmol) in toluene (1.6 ml) was added a solution of $HAuCl_4 \cdot 3\ H_2O$ (5.5 mg, 13.3 µmol) in water (0.6 ml) giving an orange solution which was stirred for 5 min. Then was added the dithiol **1** (4.5 mg, 6.2 µmol) in a small amount of toluene (0.5 ml). The mixture was stirred again for 5 min and then a solution of $NaBH_4$ (5 mg, 0.13 mmol) was added immediately giving a black suspension. The reaction mixture was stirred overnight and the organic layer washed with water (3x 2 ml). The

toluene was then removed under reduced pressure and the colloids were dried *vacuo*. The colloids were purified by dissolution in toluene (2 mL) and precipitation by the addition of MeOH (30 mL). This material was filtered, and purified by gel permeation chromatography (Sephadex LH-20, 5/1 $CHCl_3$/MeOH) and concentrated *in vacuo* to give pure gold colloids. ^{1}H NMR of this material had only broad signals. UV-Vis: (toluene) $\lambda_{max}(\varepsilon)$: 296 (28600), (20400), 351 (15200), 526 (3900); CD: (toluene) $\lambda_{max}(\Delta\varepsilon)$: 283 (+91.0), 324 (-15.8), 359 (-19.6).) 296 (28600), (20400), 351 (15200), 526 (3900); CD: (toluene) $\lambda_{max}(\Delta\varepsilon)$: 283 (+91.0), 324 (-15.8), 359 (-19.6).

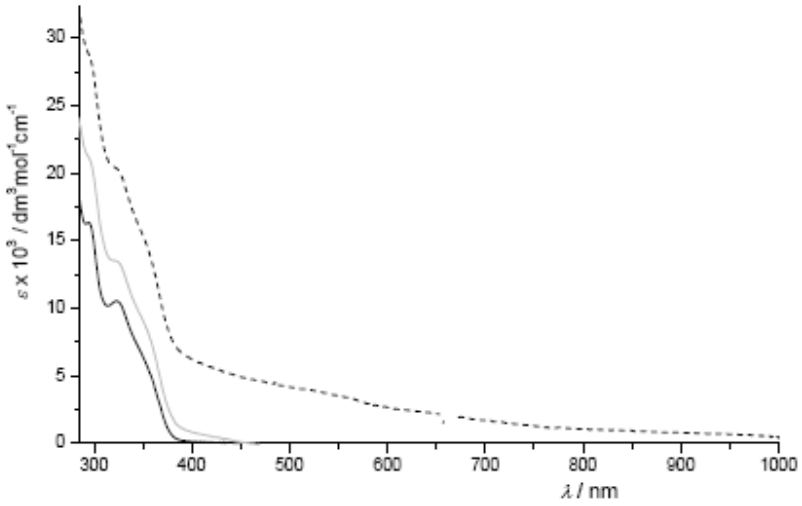

Figure 2: UV-Vis spectra of functionalised gold nanoparticles <u>1-Au</u> (dashed black) in toluene (baseline: toluene), <u>1-Au</u> (solid grey) in toluene (baseline: octanethiol functionalised gold nanoparticles in toluene) and methoxy-legged motor <u>2</u> (solid black). The UV of <u>1-Au</u> with a very weak surface plasmon band around 520 nm, characteristic for Au colloids of these dimensions[1].

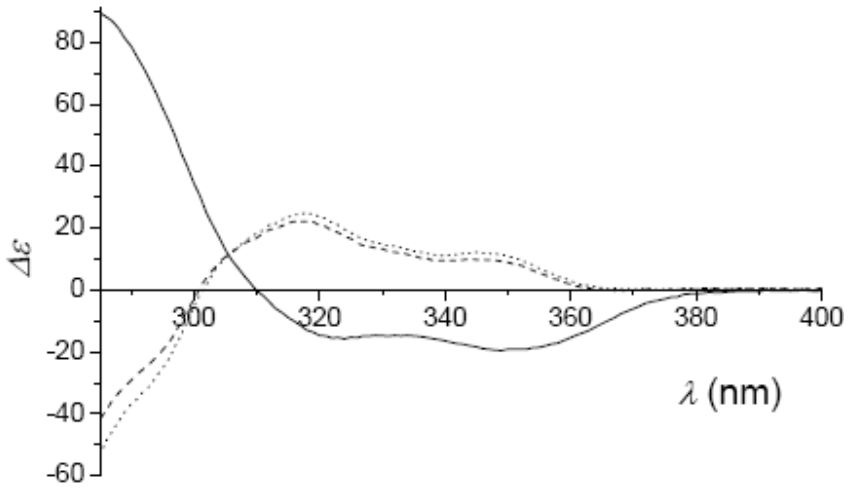

Figure 3: CD spectra of pure (2'R)-(M)-1 (solid), $PSS_{\geq 280\ nm}$ (dashed), and $PSS_{365\ nm}$ (dotted) in toluene solution. All spectra are adjusted for molar concentration of chromophores.

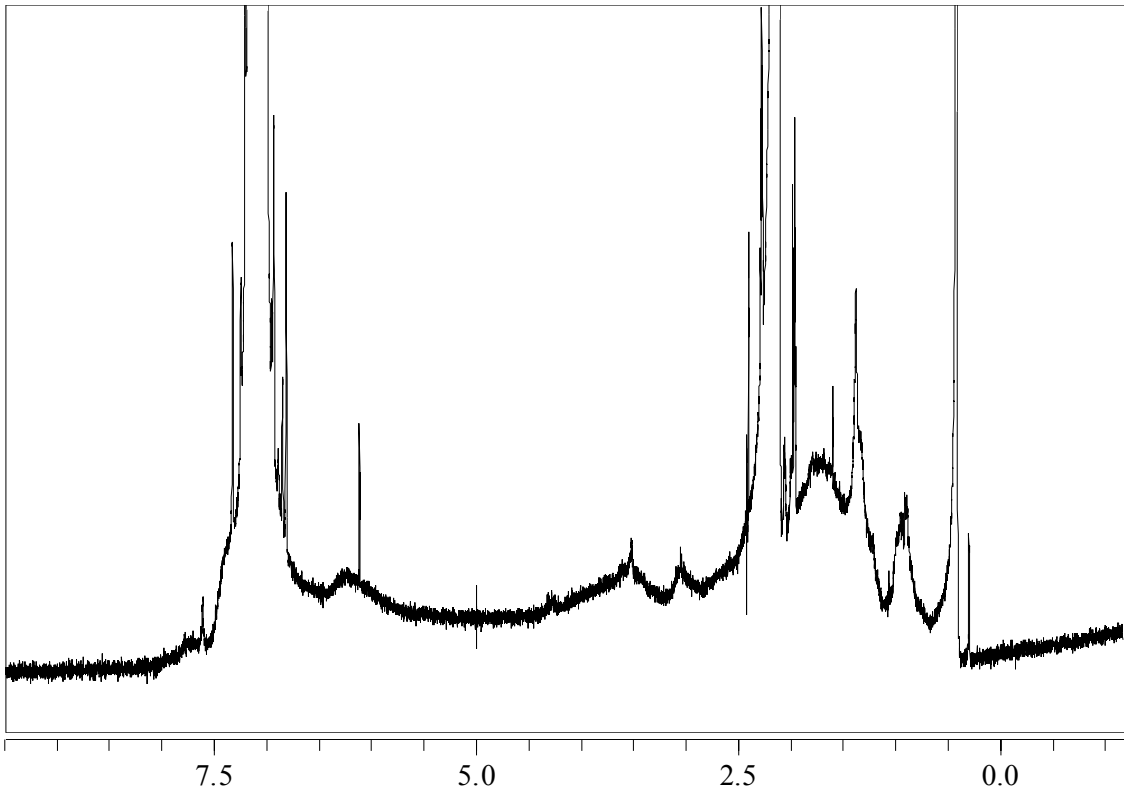

Figure 4: 400 MHz ^{1}H NMR of 1-Au. This spectrum has only broad signals replacing the signals of unbound motor molecule 1, indicating that no free motor was present.

Motor functionalised colloids 1-Au after irradiation and cleavage from the nanoparticles.

Method: **1-Au** (2 mg) in toluene (1.5 mL) was irradiated with at 280 or 365 nm light for 3 h. Etching of the gold nanoparticles was achieved by concentration of the mixture *in vacuo*, redissolution in THF (0.5 mL) and addition of a solution of KCN in water (3 mL, 2 mg/mL). The broad UV/Vis absorption of the gold plasmon had disappeared completely after 30 min. After this, the material was extracted with toluene (2 x 5 mL), concentrated *in vacuo*, and analysed by ^{1}H and ^{13}C NMR.

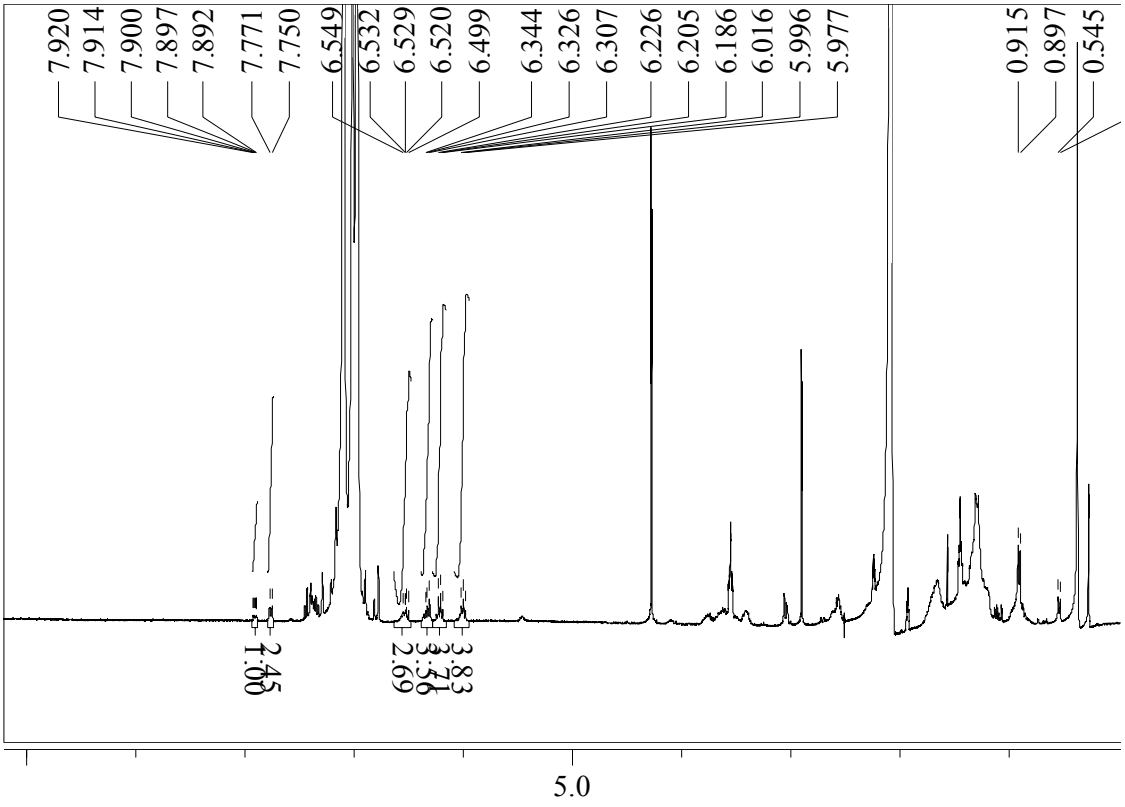

Figure 5: KCN mediated etching of the gold core of <u>1-Au</u> after 3 h irradiation revealed motor <u>1</u> as its unstable and stable isomers in a (2.5:1 ratio).

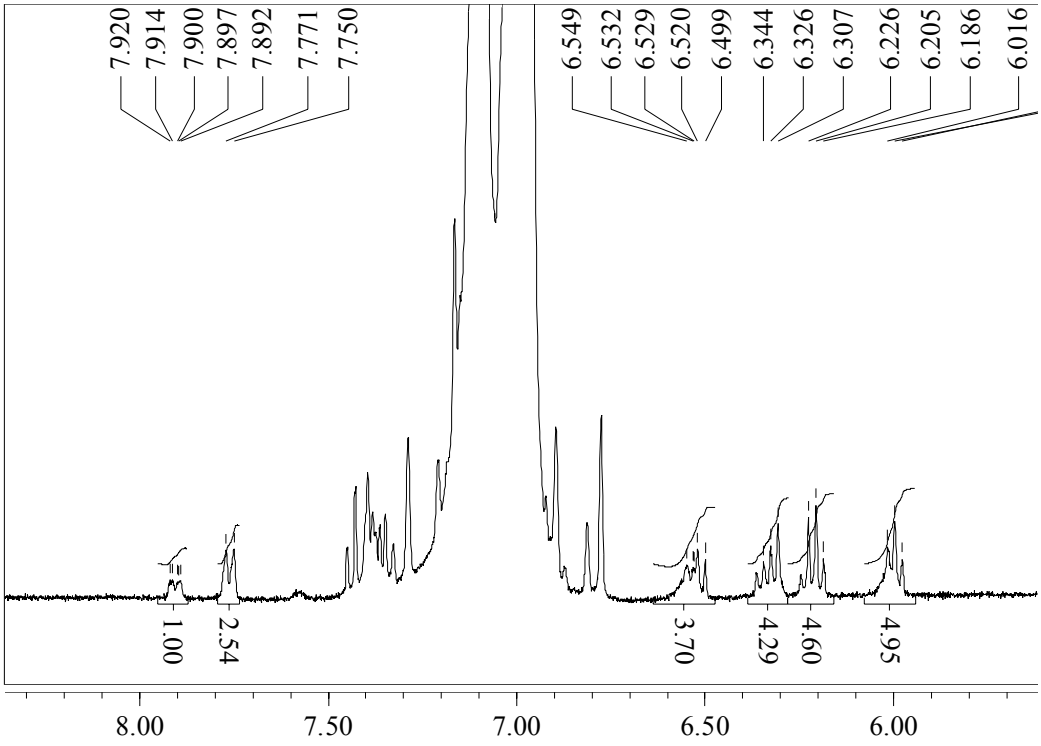

Figure 6: Expansion of 400 MHz ^{1}H NMR after irradiation of 1-Au, etching of the gold core leaving the motor free in solution, likely as a mixture of thiol and disulfide. Comparison of the integration of peaks at 7.76 (unstable isomer) and 7.91 (stable isomer) is 2.5 : 1.

Reflectance FT-IR, solid state Raman and Surface enhanced resonance Raman spectroscopic characterisation of motor derivatised Au nanoparticles.

Spectroscopic marker bands of the motor's alkyl 'legs' in the derivatised nanoparticles were used to determine the mode of binding of the motor to the gold nanoparticles. The low energy finger print region (Figure 7) of the modified nanoparticles both with dodecanethiol and motor modification show strong alkane vibrational features at 803 cm^{-1}, 1022 cm^{-1}, 1094 cm^{-1} and 1260 cm^{-1}. They confirm that in both cases long alkyl chains are present in the modified nanoparticles. The strong aliphatic C-H vibrations observed <3000 cm^{-1} support this assignment. By examination of the high energy

fingerprint region of the IR spectra (Figure 8) it is clear that the aromatic C=C stretching vibrations of the motor (1571/1558 cm^{-1}) and the very weak C-H vibrations >3000 cm^{-1} (Figure 9) are present in the motor modified nanoparticles and are unaffected by the modification suggesting non specific binding of the motor to the gold surface does not occur (see Raman section below). The absence of these vibrational bands in the IR spectrum of the dodecanethiol modified nanoparticles supports this assignment.

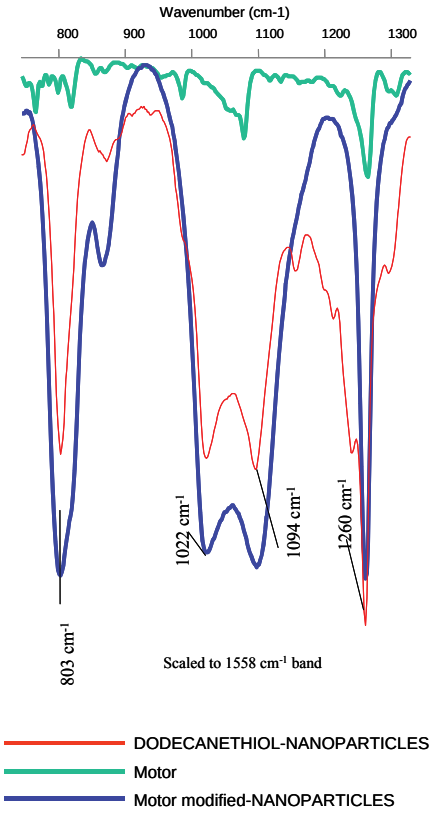

Figure 7: Overlay of low energy fingerprint region in FT-IR spectrum of motor, dodecanethiol modified nanoparticles and motor modified nanoparticles.

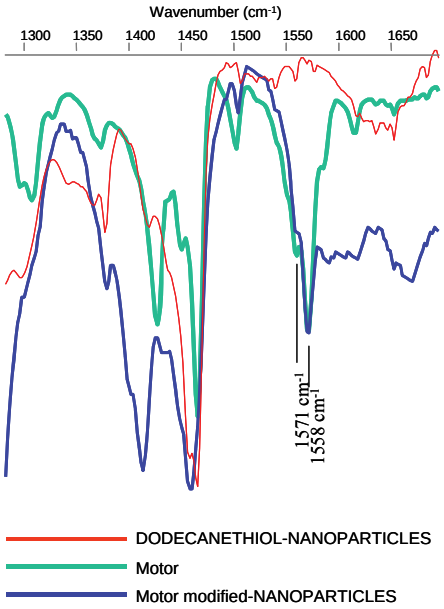

Figure 8: Overlay of high-energy finger print region in FT-IR spectrum of motor, dodecanethiol modified nanoparticles and motor modified nanoparticles.

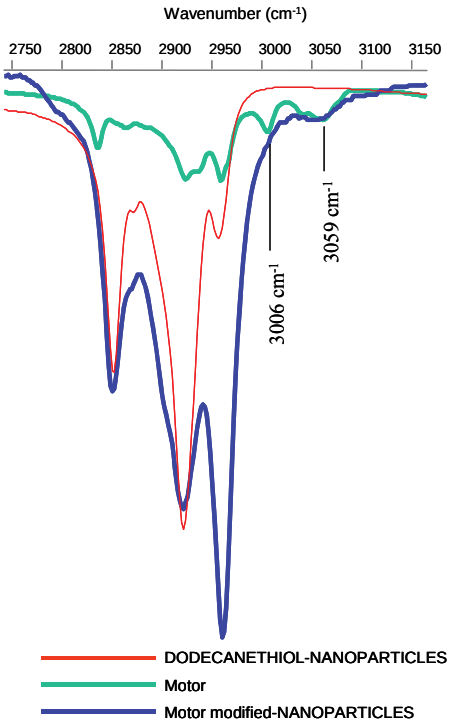

Figure 9: Overlay of C-H stretching region of FT-IR for motor, dodecane thiol modified nanoparticles and motor modified nanoparticles.

Solid state Raman and surface enhanced resonance Raman spectroscopy: evidence for vibrational perturbation by non-specific binding to gold nanoparticles

In Figure 10, the solid state Raman spectrum and the SERS spectrum of the motor are presented. The very large changes in vibrational structure in the SERS spectrum compared with the solid state spectrum imply that the interaction of the motor with the gold nanoparticles in the SERS experiments results in considerable perturbation of the molecular structure, presumably through interaction of the thioether and alkene moieties with the gold surface. The absence of significant changes to the vibrational features (in particular the C=C vibrations around 1500-1600 cm^{-1}) in the IR spectra of the modified nanoparticles supports the conclusion that the binding mode of the motors to the nanoparticles is via the alkylthiol 'legs' and that non-specific interactions of the motor with the gold nanoparticles surface do not occur to a significant degree.

Surface enhanced resonance Raman spectroscopic characterisation of motor derivatised Au nanoparticles

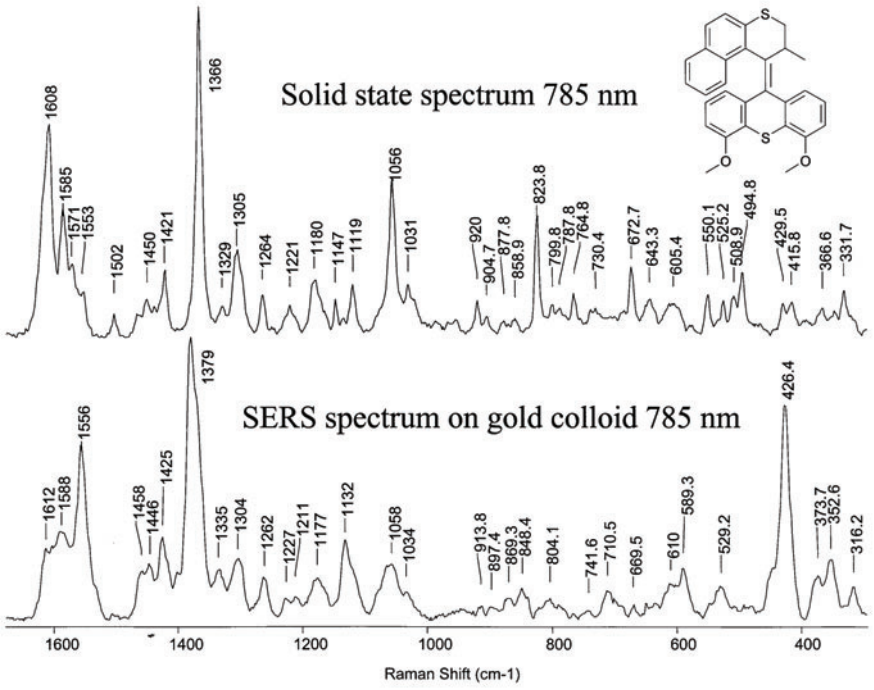

Figure 10: **Solid state Raman (upper) and surface enhanced Raman {on Au} (lower) spectra of motor recorded at 785 nm.**

Non-specific adsorption of the olefin via the thioether moieties was further excluded by control experiments with motor molecules lacking the octylthiol legs, which did not result in stable nanoparticles.

TEM studies

Representative TEM images (left, Figure 11) of capped gold nanoparticles **1-Au** deposited on an amorphous carbon film by drop-casting from a dilute toluene solution and the corresponding particle size distribution derived from digital analysis of 1246 particles. The nanoparticles are well-dispersed and spherical in shape with an average

core diameter of 2.0 nm, corresponding to 251 Au atoms, with a distribution range of 1.5 - 4.0 nm (right, Figure 11).

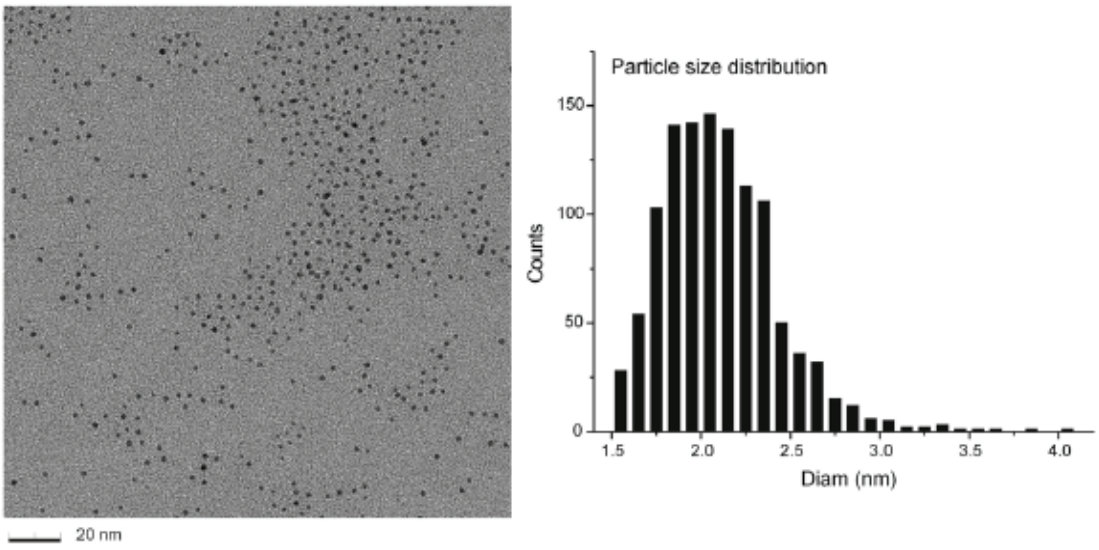

Figure 11: Representative TEM (left) and calculated particle size distribution (right) of 1-Au.

Dynamic Light Scattering

In order to corroborate the size of the functionalised gold colloid determined by TEM, dynamic light scattering (DLS) measurements were performed at 30.0 ºC at a wavelength (λ_o) of 633.3 nm. For the measurements a solution containing 3.1 mg of nanoparticles in 1 mL of toluene was used. Prior to measurement, the samples were centrifuged for 5 min at 3000 rpm to remove any interfering dust particles from the scattering volume. The intensity mean particle size or dynamic diameter was 6.3 nm with a Gaussian-like size distribution (the intensity autocorrelation functions were analyzed using CONTIN[2]).

Section 2: This section describes characterization of compound **2.**

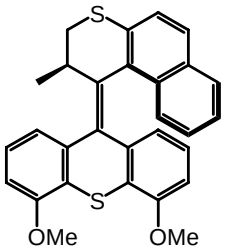

4,5-Dimethoxy-9-(2',3'-dihydro-2'-methyl-1'*H*-naphtho[2,1-*b*]thiopyran-1'-ylidene)-9*H*thioxanthene (2)

^{1}H NMR ($CDCl_3$, 400 MHz) δ 0.74 (d, *J* = 6.6, 3H, CH_3), 3.07 (dd, *J* = 11.4, 2.9 Hz, 1H, CH_2), 3.69 (dd, *J* = 11.4, 7.3 Hz, 1H, CH_2), 3.81 (s, 3H, OCH_3), 4.00 (s, 3H, OCH_3), 4.11 (m, 1H, CH), 6.06 (dd, *J* = 7.7, 1.1 Hz, 1H), 6.29 (dd, *J* = 8.1, 1.1 Hz, 1H), 6.38 (m, 1H), 6.87 (dd, *J* = 8.1, 1.1 Hz, 1H), 7.02 (m, 1H), 7.0113 (m, 1H), 7.22 (dd, *J* = 7.7, 1.1 Hz, 1H), 7.37 (m, 1H), 7.41 (d, *J* = 8.4 Hz, 1H), 7.57 (d, *J* =8.4 Hz, 1H), 7.60 (d, *J* = 8.4 Hz, 1H), 7.63 (d, *J* = 8.4 Hz, 1H); ^{1}H NMR (toluene-D_8, 400 MHz, stable isomer, axial methyl substituent) δ 0.53 (d, *J* = 6.6 Hz, 3H, CH_3), 2.69 (dd, *J* = 11.5, 2.7 Hz, 1H, CH_2), 3.22 (s, 3H, OCH_3), 3.36 (s, 3H, OCH_3), 3.38 (m, 1H, CH_2), 4.06-4.10 (m, 1H, CH), 5.87 (d, *J* = 8.1 Hz, 1H), 6.18 (m, 1H), 6.32 (d, *J* = 7.0 Hz, 1H), 6.40 (d, *J* = 8.1 Hz, 1H), 6.89 (m, 1H), 6.97-7.09 (m, 2H), 7.15 (d, *J* = 7.7 Hz, 1H), 7.31-7.37 (m, 3H), 7.88 (d, *J* = 8.4 Hz, 1H); ^{1}H NMR (toluene-D_8, 400 MHz, unstable isomer, equatorial methyl substituent) δ 0.89 (d, *J* = 7.0 Hz, 3H, CH_3), 2.26 (m, 1H, CH_2), 2.98-3.05 (m, 2H, CH_2+CH), 3.22 (s, 3H, OCH_3), 3.34 (s, 3H, OCH_3), 5.86 (d, *J* = 8.1 Hz, 1H), 6.16 (m, 1H), 6.29 (d, *J* = 7.7 Hz, 1H), 6.36 (m, 1H), 6.90-7.16 (m, 4H), 7.36-7.44 (m, 3H), 7.74 (d, *J* = 8.1 Hz, 1H); ^{13}C NMR ($CDCl_3$, 75 MHz) δ 19.1 (q), 32.0 (d), 37.2 (t), 56.0 (2xq), 107.6 (d), 108.2 (d), 119.9 (d), 121.6 (d), 122.7 (s), 124.3 (d), 124.5 (d), 125.4 (d), 125.5 (d), 125.7 (d), 126.5 (d), 127.3 (d), 127.4 (d), 130.8 (s), 131.3 (s), 131.6 (s), 132.2 (s), 134.7 (s), 136.3 (s),

136.5 (s), 138.8 (s), 155.2 (s), 156.1 (s), one (s) signal was not observed; m/z (EI, %) = 468 (M^+, 100); HRMS (EI): calcd. for $C_{29}H_{24}O_2S_2$: 468.1218, found 468.1208. Resolution of (2'*R*)-(*M*)-**2** and (2'S)-(*P*)-**2** was achieved by preparative chiral HPLC employing a Chiralcel AD column as the stationary phase and *n*-heptane : *i*-propanol 9:1 as the eluent (1 mL·min^{-1}). The first eluted fraction (t = 5.1 min) was assigned by CD spectroscopy to be (2'*R*)-(*M*)-**2** and second eluted fraction (t = 6.4 min) was assigned to be (2'*S*)-(*P*)-**2**. The fraction containing the (2'*R*)-(*M*) isomer of **2** was used for all chiroptical studies on compound. The absolute configuration of the molecule chosen for the molecule was determined by Flack's refinement (x = 0.01(5); UV-Vis and CD spectroscopic data for pure stable (2'*R*)-(*M*)-**2**: UV-Vis: (toluene) $\lambda_{max}(\varepsilon)$ 295 (16300), 323 (10500), 350 (shoulder, 6400); CD: (toluene) $\lambda_{max}(\Delta\varepsilon)$ 283 (+92.6), 322 (-15.2), 351 (-18.6); CD: (*n*-dodecane) $\lambda_{max}(\Delta\varepsilon)$202 (+31.4), 214 (-67.5), 241 (-5.4), 251 (-46.0), 281 (+92.0), 321 (-14.8), 349 (-18.8); UV-Vis and CD spectroscopic data for pure unstable (2'R)-(P)-**2**: UV-Vis (calc., toluene) $\lambda_{max}(\Delta\varepsilon)$ 295 (16900), 315 (10900), 347 (shoulder, 3900); CD: (calc., toluene) $\lambda_{max}(\Delta\varepsilon)$ 283 (-66.0), 318 (+26.2), 345 (+13.5)

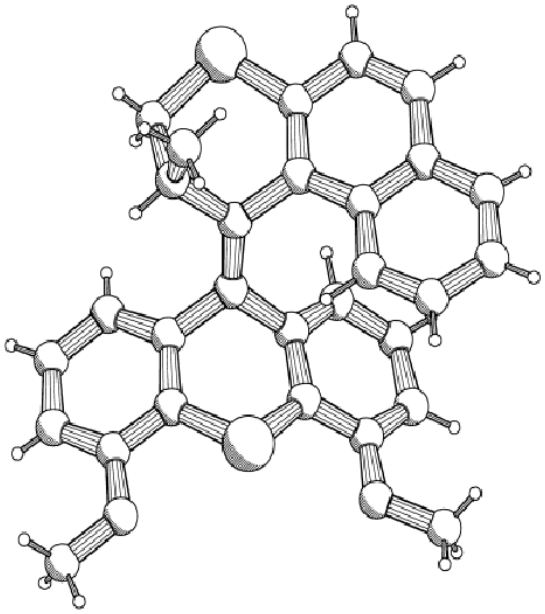

formula	$C_{29}H_{24}O_2S_2$	ρ (g·cm^{-3})	1.309
fw (g·mol^{-1})	468.64	T (K)	110(2)
crystal dimension (mm)	0.13 x 0.11 x 0.09	μ (cm^{-1})	2.49
color, habit	colorless, parallelpiped	number of reflections	11841
crystal system	monoclinic	number of refined	
space group, no.	$P2_1$, 4	parameters	786
a (Å)	8.9625(6)	final agreement factors:	
b (Å)	22.785(2)	$wR(F^2)$	0.0863
c (Å)	11.6435(8)	$R(F)$	0.0420
β (°)	90.127(1)	GooF	1.036
V (Å^3)	2377.7(3)	Flack's refiment	0.01(5)
Z	4		

Table 1: X-Ray crystallographic data for (2'*R*)-(*M*)-2.

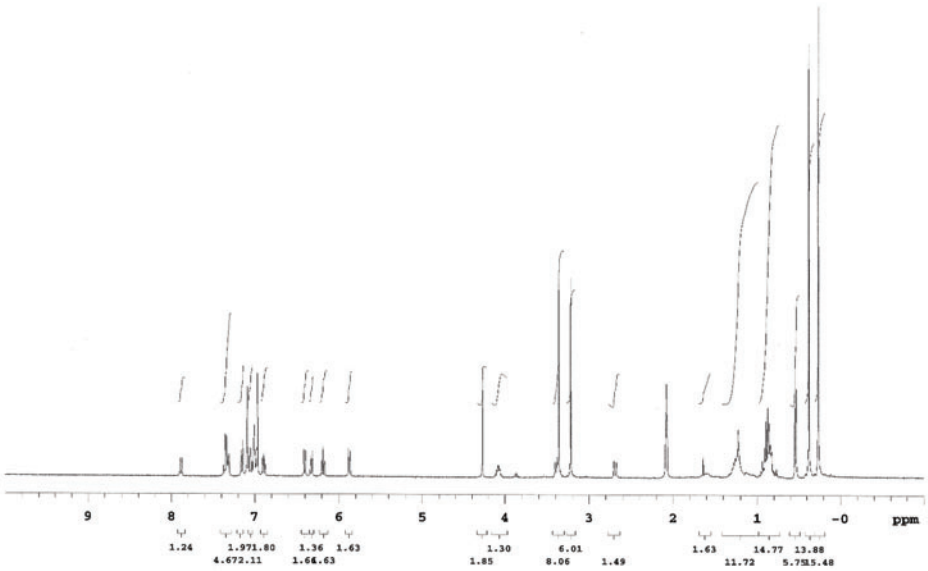

Figure 12: 400 MHz ^{1}H NMR of 2.

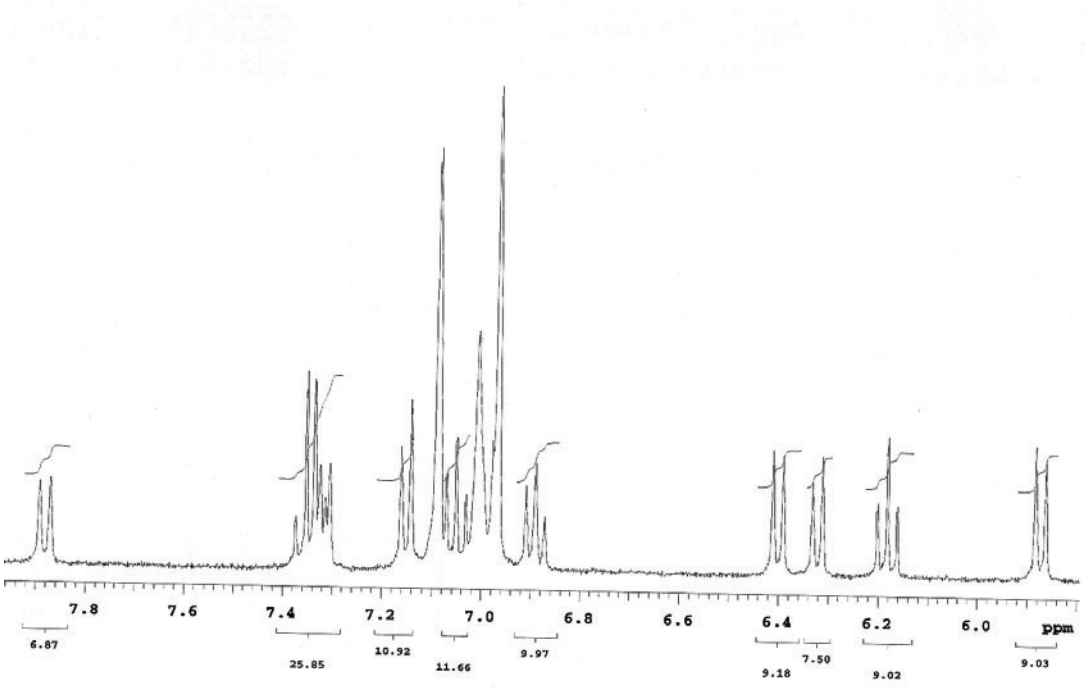

Figure 13: 400 MHz ^{1}H NMR of 2, expansion to show crucial reporter peak at 7.88 ppm.

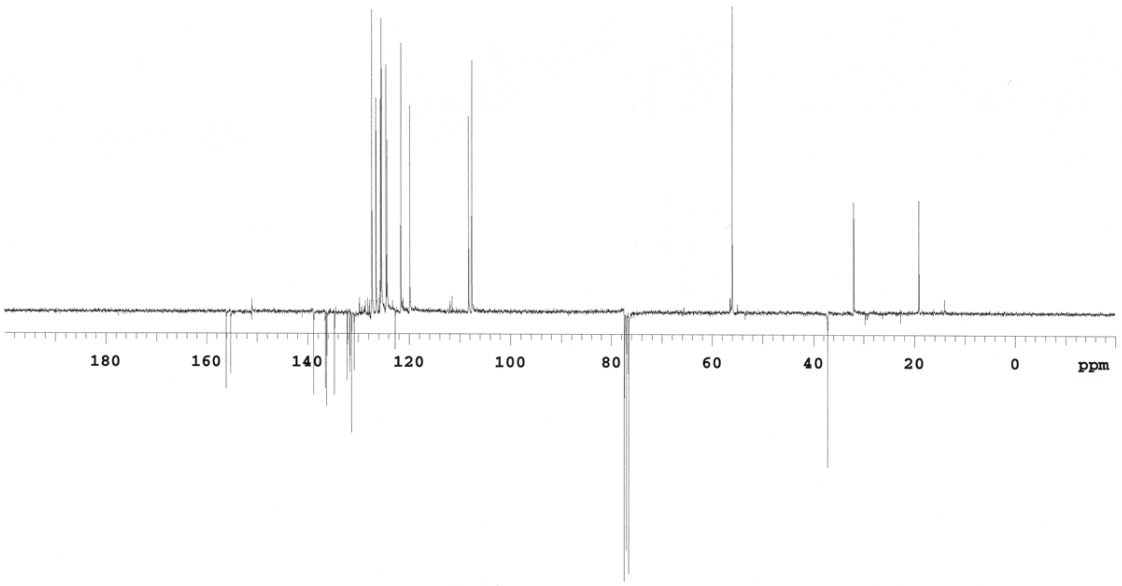

Figure 14: 100 MHz APT spectrum of 2 in $CDCl_3$.

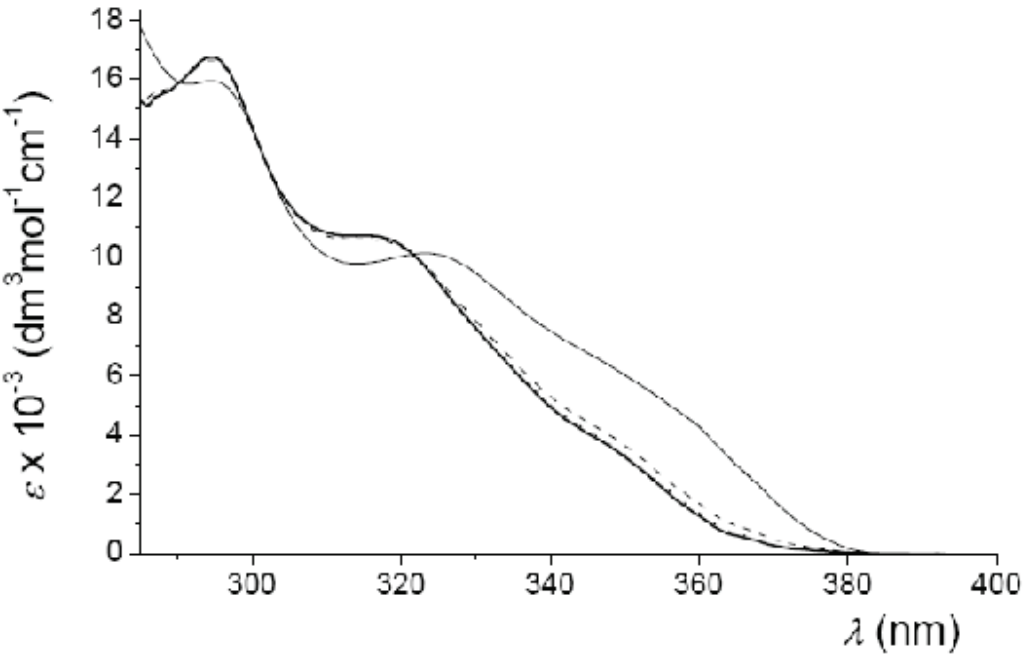

Figure 15: UV-Vis spectra of pure (2'*R*)-(*M*)-2 (solid line), $PSS_{\geq 280\ nm}$ (dashed line), $PSS_{365\ nm}$ (dotted line) and the calculated UV-Vis spectrum of (2'*R*)-(*P*)-2 (thick solid line) recorded in toluene.

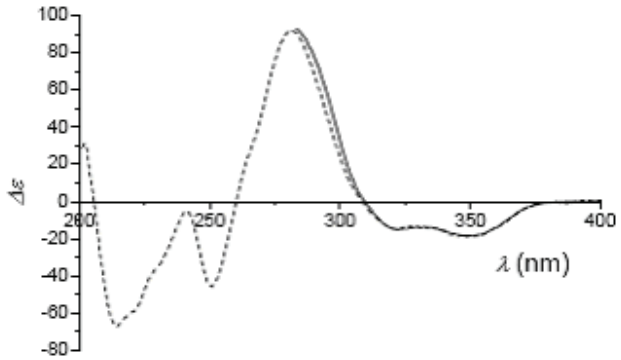

Figure 16: CD spectra of dimethoxy substituted motor 2 in toluene (solid line) and dodecane (dashed line).

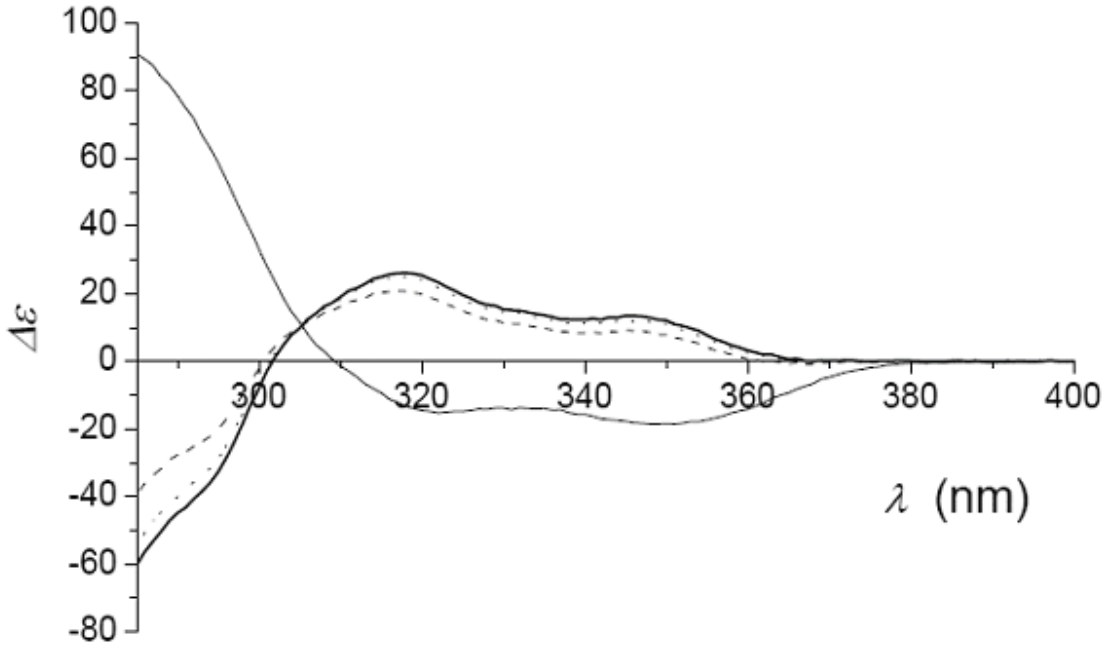

Figure 17: CD spectra of pure (2'*R*)-(*M*)-2 (solid black), $PSS_{\geq 280\ nm}$ (dashed black), $PSS_{365\ nm}$ (dotted black) and the calculated CD spectrum of (2'*R*)-(*P*)-2 (thick black) recorded in toluene.

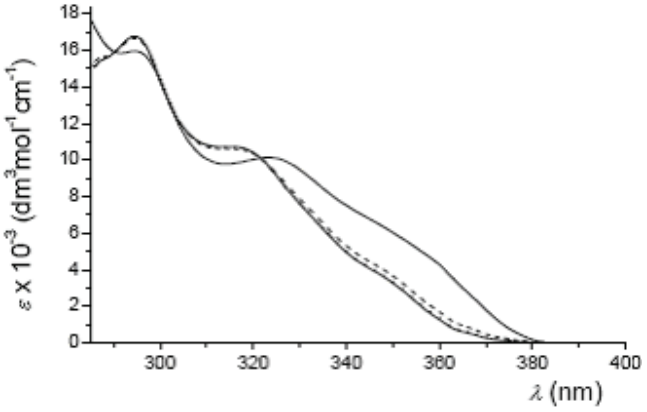

Figure 18 UV-Vis spectra of pure (2'*R*)-(*M*)-2 (solid line), $PSS_{\geq 280\ nm}$ (dashed line), $PSS_{365\ nm}$ (dotted line) and the calculated UV/Vis spectrum of (2'*R*)-(*P*)-2 (thick solid line, based on correlating 94:6 unstable/stable in NMR studies with observed UV) recorded in toluene.

*Section 3: This section describes experiments designed to verify that **2** behaves as a unidirectional molecular motor. This was achieved by replacing the CH_3 group with a CD_3 group to allow distinction between cis and trans diastereomers. The experiments performed on the cis-**3** exclude any alternative mechanisms to explain the data observed for **1**, involving either photochemical helix inversion without isomerisation and/or thermal isomerisation.*

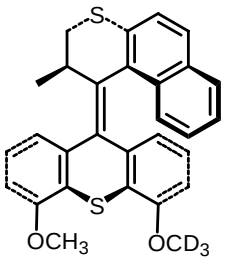

4-Methoxy(D_3)-5-methoxy-9-(2',3'-dihydro-2'-methyl-1'*H*-naphtho[2,1-*b*]thiopyran-1'-ylidene)-9*H*-thioxanthene (3)

According to ^{1}H NMR, the *cis-trans* ratio of the enriched product for study was 80:20. The ^{1}H and ^{13}C NMR spectra were identical to the previously synthesized all hydrogen analogue **2**, except for the methoxy signal (which had a 4/1 relative integration for signal from the expected methoxy CH_3); *m/z* (EI, %) = 471 (M^+, 100); HRMS (EI): calcd. for $C_{29}D_3H_{21}O_2S_2$: 471.1403, found: 471.1410.

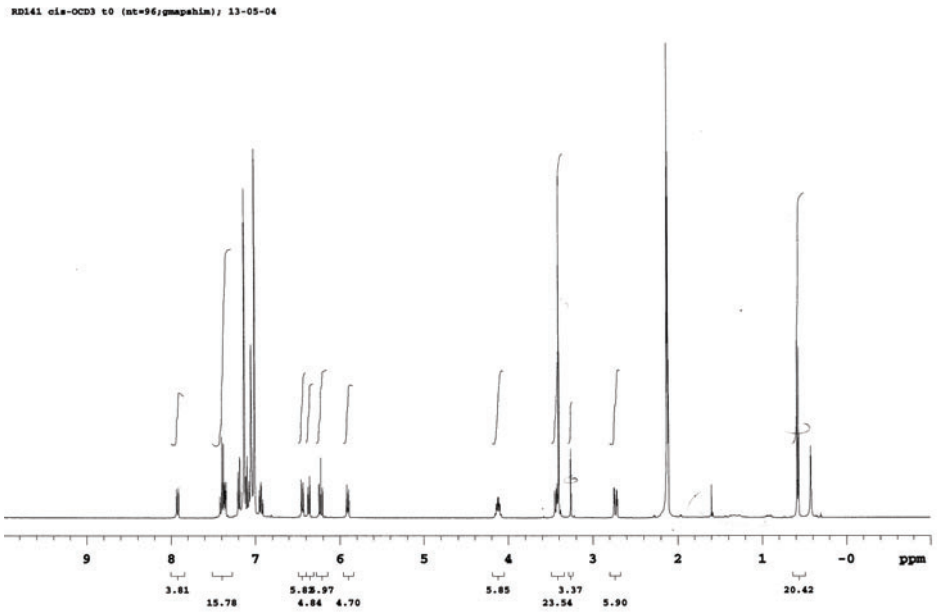

Figure 19: 400 MHz ^{1}H NMR spectrum of 3.

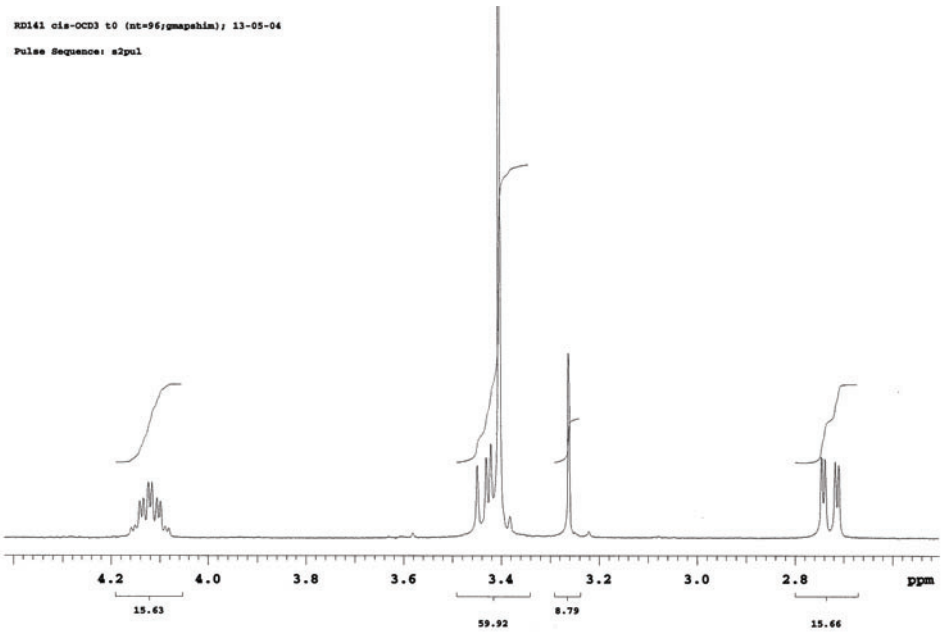

Figure 20: Expansion of 400 MHz ^{1}H NMR of 3.

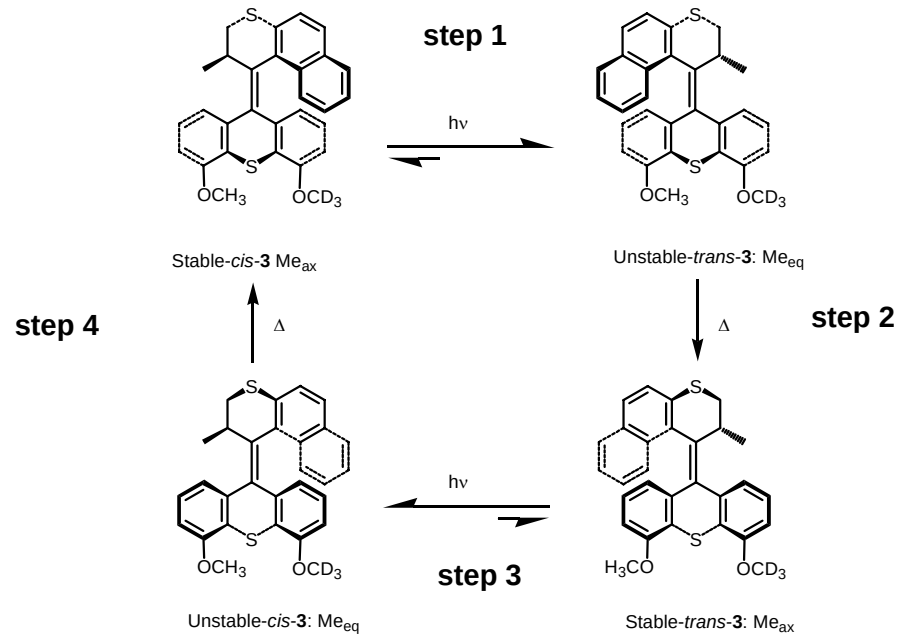

Figure 21: Unidirectional rotation was demonstrated by comparing the conversion of the stable form of 3 to the unstable form, with the conversion of *cis* to *trans*.

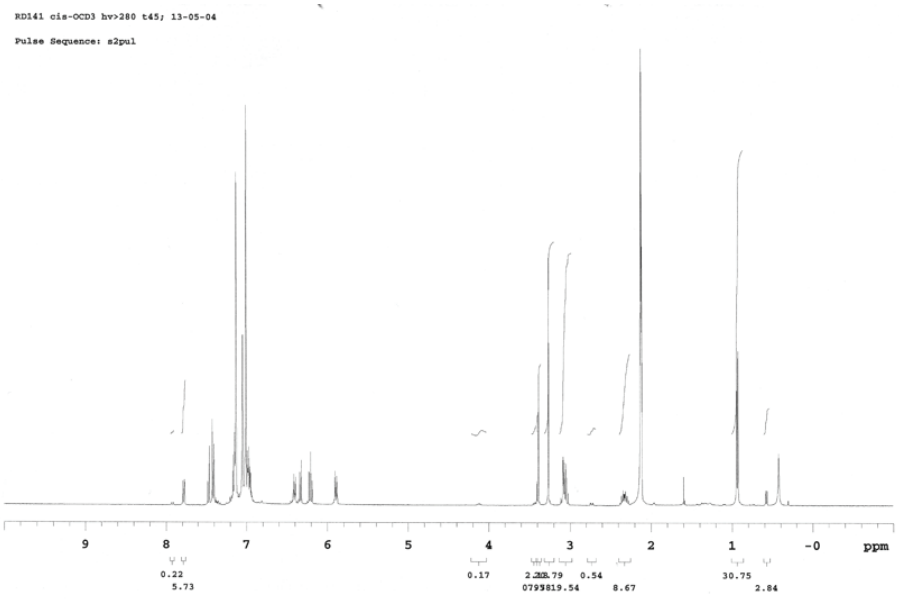

Figure 22: A sample consisting of 80% stable-*cis*-3 and 20% unstable-*trans*-3 was irradiated ($\lambda \geq 280$ nm) generating a mixture 73:18 : 7:2 of unstable-*trans*-3, unstable-*cis*-3, stable-*cis*-3 and stable-*trans*-3. This is consistent with 90% conversion of each of isomers to their corresponding unstable forms, which is supported by the change in the signals from the methoxy groups.

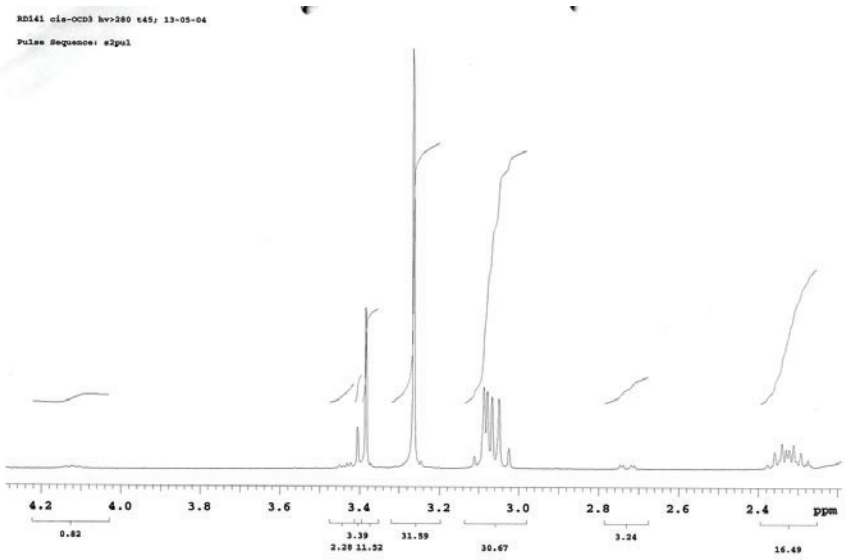

Figure 23: The expansion of the 400MHz ^{1}H NMR of an irradiated sample of 80% enriched stable-*cis*-3 revealed a ratio of *cis/trans* by relative integrations of methoxy protons. The absorptions of the methoxy groups shift only slightly and overlap with protons of the upper half. 73:18 : 7: 2.

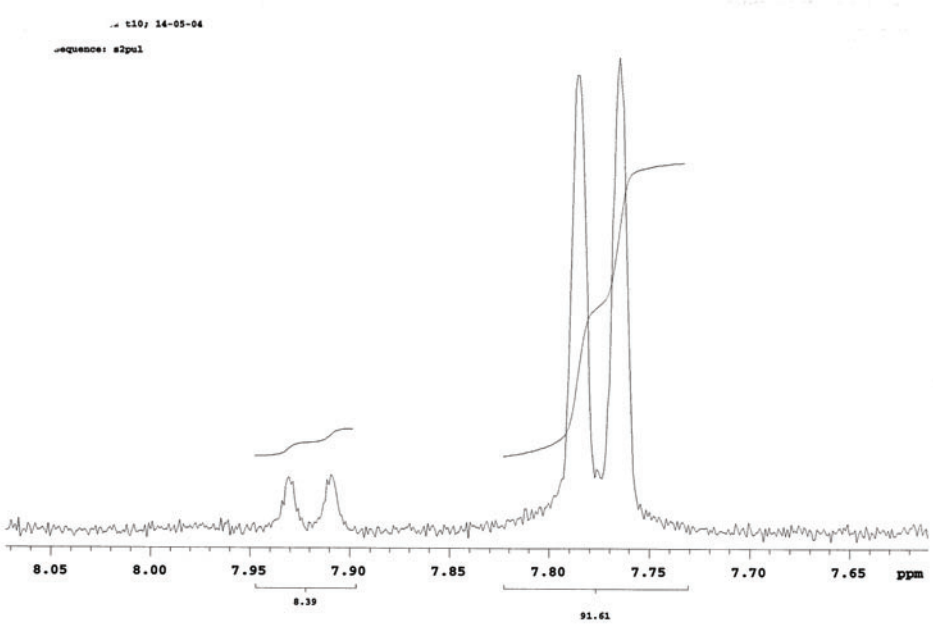

Figure 24: Expansion of 400 MHz ^{1}H NMR of the $PSS_{>280}$ of 3, revealing a mixture of starting material stable isomers (left doublet, 9% total) and a mixture of the unstable isomers unstable-*trans*-3 and unstable-*cis*-3 (right doublet, 91 % total).

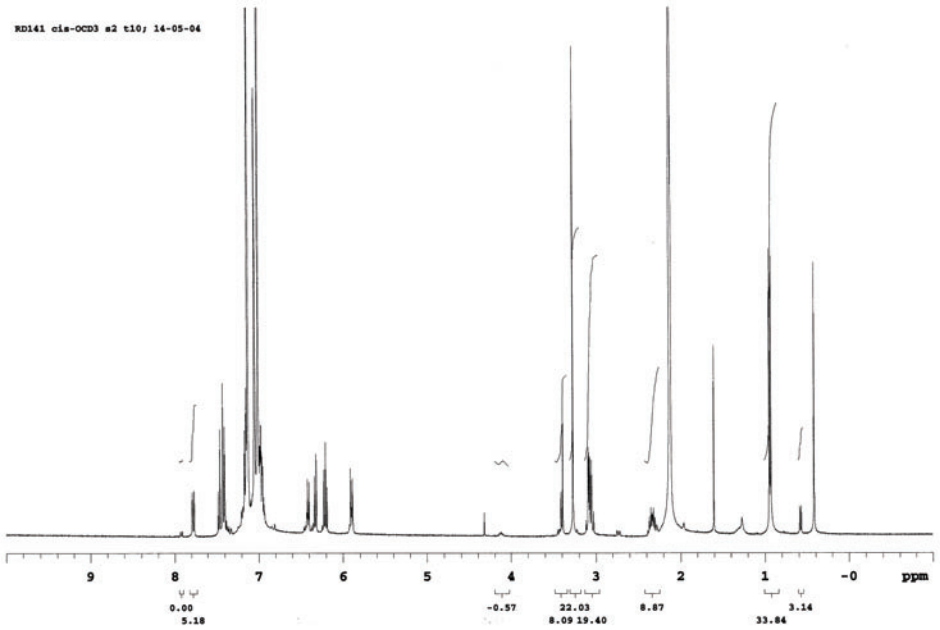

Figure 25: 400 MHz ^{1}H NMR of PSS$_{>280nm}$ of irradiated 80% enriched *cis*-3.

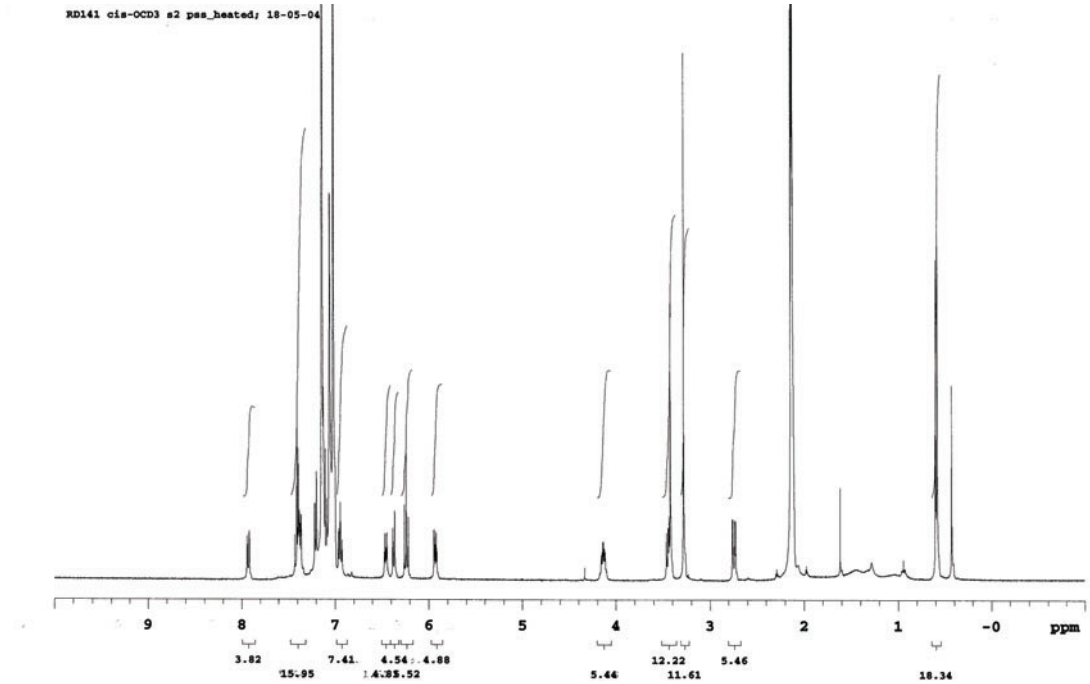

Figure 26: 400 MHz ^{1}H NMR of PSS$_{280nm}$ of irradiated *cis*-3 after heating to 70 °C to complete the thermal helix inversion. The spectrum shows complete conversion of unstable-*trans*-3 and unstable-*cis*-3 to stable-*trans*-3 and stable-*cis*-3 respectively. The *cis/trans* ratio after irradiation and subsequent heating was determined by ^{1}H NMR to be 25:75 (*CIS*: 7% remaining from starting *cis*-3 plus 18% from isomerised unstable-*trans*-3; *TRANS*: 71% from isomerised unstable-*cis*-3, and 4%

from starting material stable-*trans*-3). This is consistent with the ratio of isomers expected for a unidirectional rotary process.

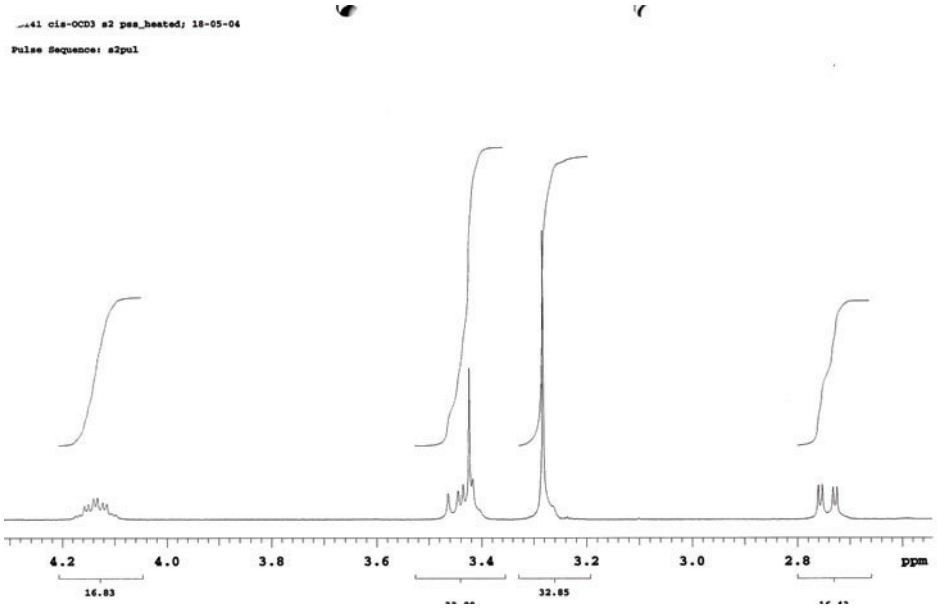

Figure 27: 400 MHz ^{1}H NMR of PSS_{280nm} of irradiated *cis*-3 after heating for 70 °C to complete the thermal helix inversion.

Section 4

This section describes data from experiments designed to verify that **1** behaves as a unidirectional molecular motor while attached to the gold colloid, **1-Au**. This was achieved by ^{13}C isotope enrichement of the ether carbon of one "leg" which allowed the distiction between *cis* and *trans* diastereomers (*cis*-**4** and *trans*-**4** respectively). The experiments performed on *cis*-**4** and *cis*-**4-Au** are described below.

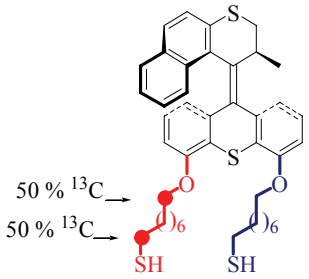

^{13}C-Labelled 4,5-bis[(8-sulfanyloctyl)oxy]-9-(2',3'-dihydro-2'-methyl-1'*H*-naphtho[2,1-b]thiopyran-1'-ylidene)-9*H*-thioxanthene (*cis*-4)

^{1}H NMR (400 MHz, $CDCl_3$) δ 0.74 (d, J = 7.2 Hz, 3H), 1.20-1.65 (m, 20H), 1.72-1.79 (m, 2H), 1.92 (quin, J = 6.9 Hz, 2H), 2.88 (m, 3H), 2.88 (dt, $^{3}J_{HH}$ = 7.4 Hz, $^{1}J_{CH}$ = 141 Hz, 1H, $^{13}CH_2SH$,), 3.08 (dd, J = 11.4, 2.6 Hz, 1H), 3.72 (dd, J = 11.2, 7.6 Hz, 1H), 3.63-4.00 (m, 2H), 4.00-4.19 (m, 3H), 6.01 (d, J = 7.6 Hz, 1H), 6.26 (AB doublet, 1H), 6.33 (ABX triplet, 1H), 6.83 (d, J = 8.0 Hz, 1H), 6.98 (t, J = 8.0 Hz, 1H), 7.09 (t, J = 7.4 Hz, 1H), 7.19 (d, J = 7.8 Hz, 1H), 7.28 (t, J = 8.0 Hz, 1H), 7.34 (d, J = 8.8 Hz, 1H), 7.49-7.59 (m, 3H), SH not observed.

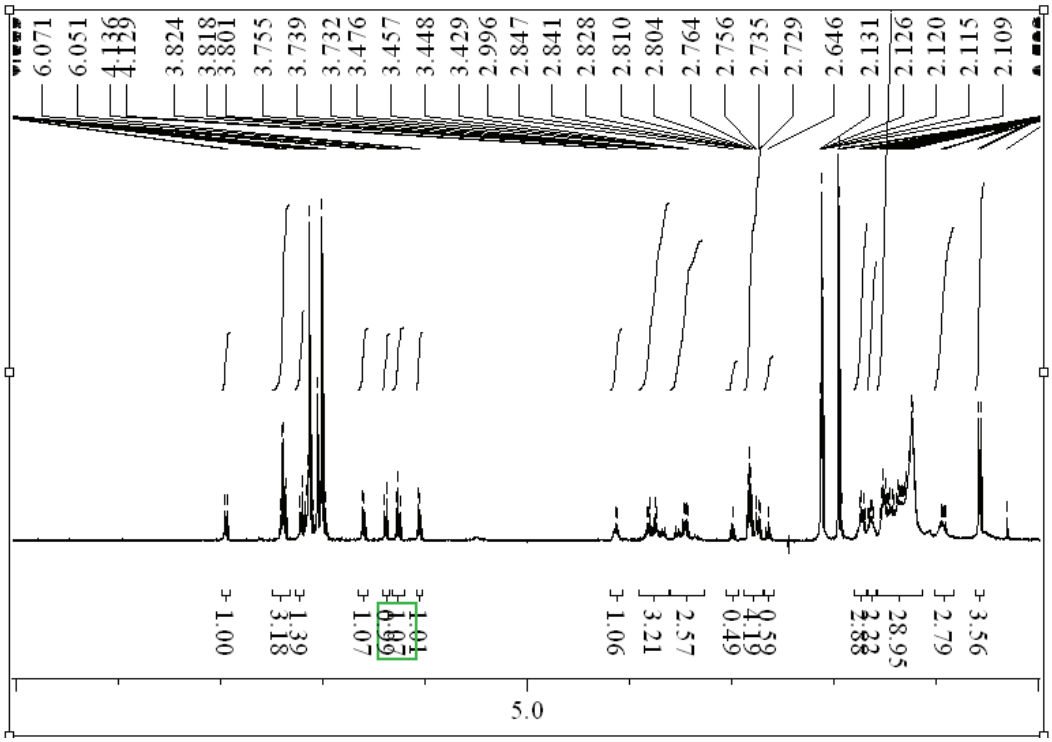

Figure 28: 400 MHz ^{1}H NMR spectrum of *cis*-4.

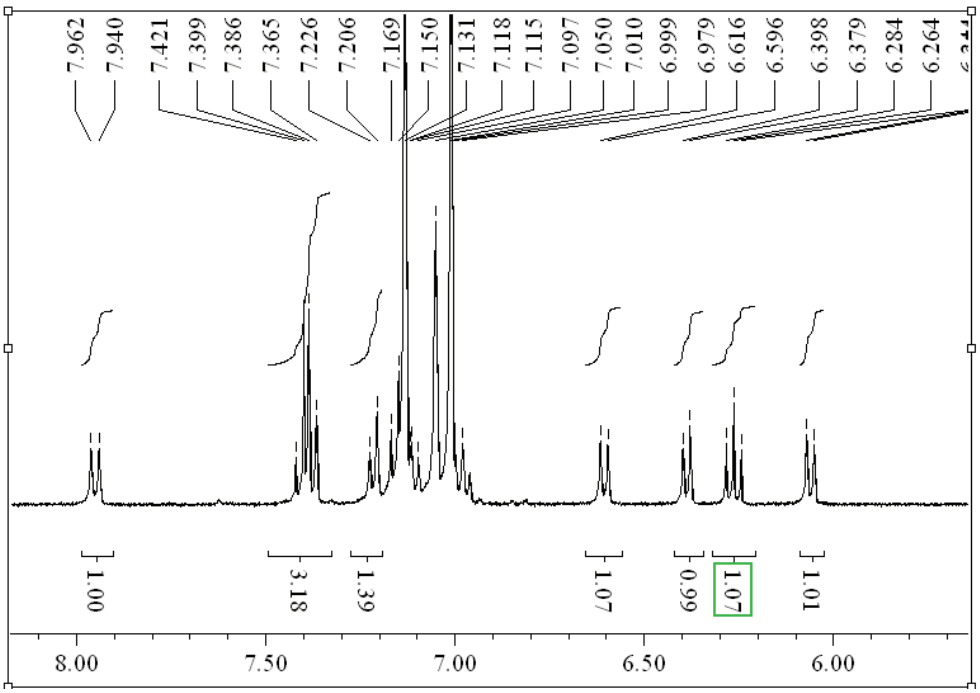

Figure 29: Expansion of the key region in the 400 MHz ^{1}H NMR spectrum of *cis*-4.

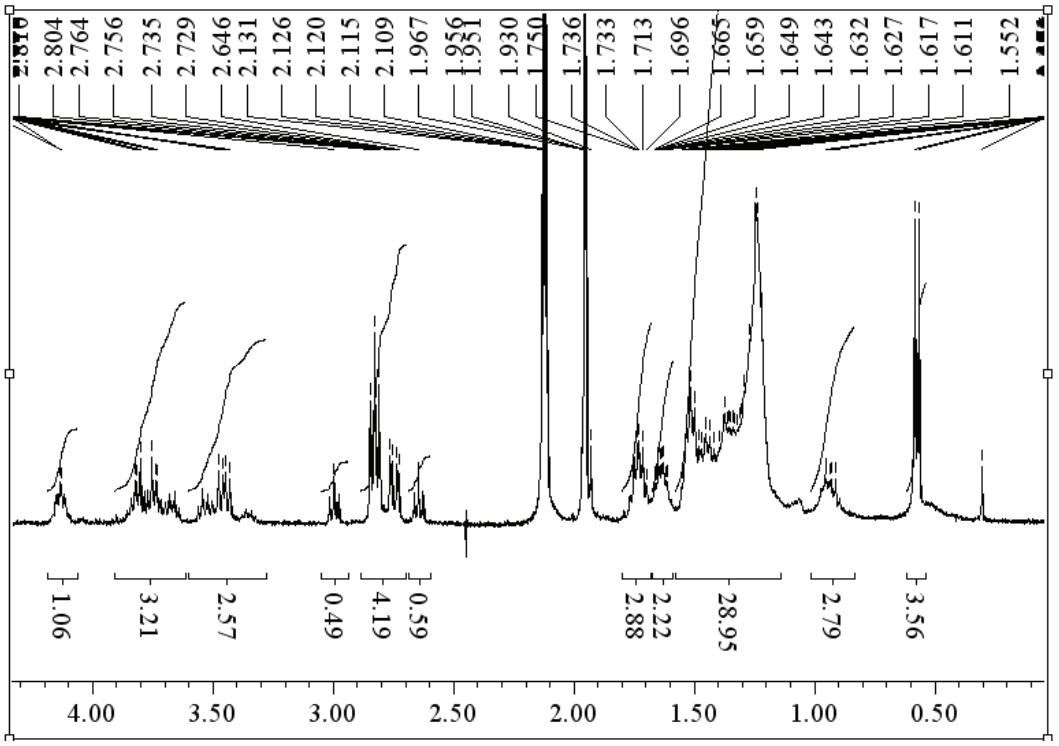

Figure 30: Expansion of 400 MHz ^{1}H NMR spectrum of *cis*-4.

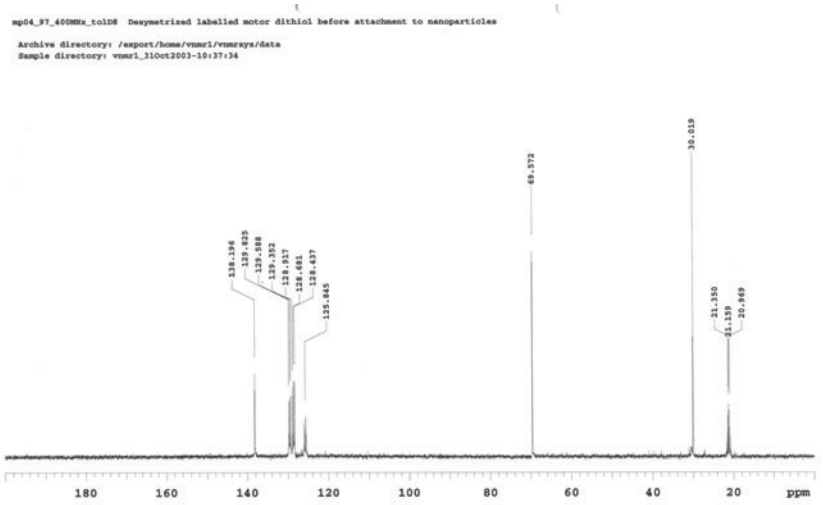

Figure 31: 400 MHz ^{13}C NMR spectrum in Toluene $D_{8\ of}$ *cis*-4. Note spectrum is not referenced to toluene D_8. $PhD_5\underline{C}D_3$ should be shifted 0.76 ppm downfield from 21.6 to 20.4 ppm, shifting the $O^{13}\underline{C}H_2$ resonance at 68.9 ppm.

Experiments with ^{13}C labeled motor functionalised nanoparticles 4-Au to demonstrate unidirectional rotation on gold

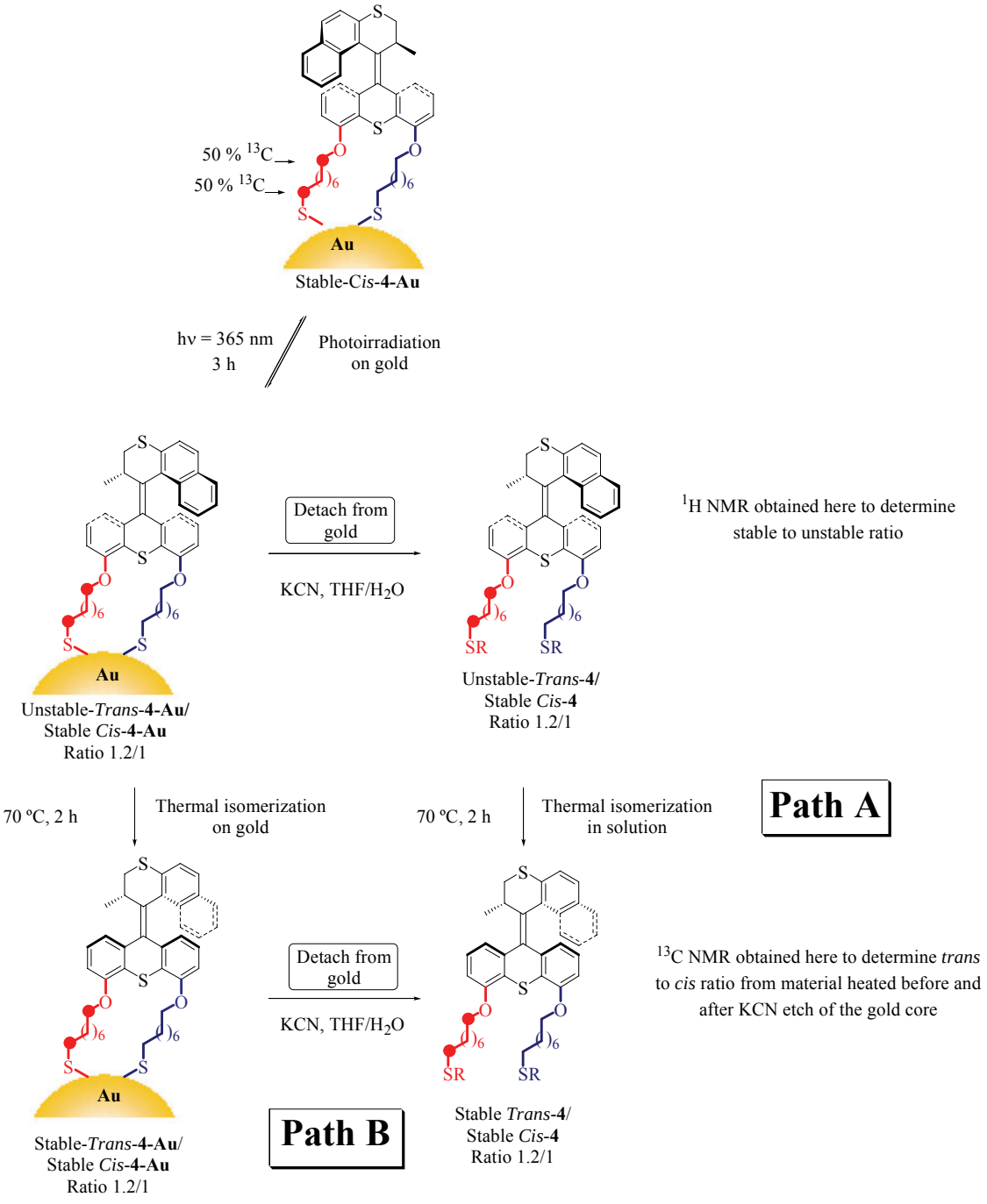

Figure 32: Depiction of the two experiments performed on 4-Au.

Gold colloids **4-Au** were prepared and purified from *cis*-**4** using an analogous procedure as for **1-Au**. These colloids were irradiated at 365 nm for 3 h at with vigorous stirring in a cuvette in toluene (Figure 32). This sample was split into two portions. The first (Path A) was reduced *in vacuo,* and treated with aqueous KCN/THF (5 mL, 1 mg/mL in THF/H_2O, 5/1). After 30 minutes the colour associated with the colloids had completely disappeared. This sample was extracted with toluene, dried, concentrated *in vacuo* and analyzed by ^{1}H NMR. This mixture was then heated at 70 °C for 2 h, and analyzed by ^{1}H NMR and ^{13}C NMR. The second portion of irradiated *cis*-**4-Au** was heated while the motor was still on the nanoparticle (Path B). These nanoparticles were
etched with KCN as described for Path A, and analyzed by ^{1}H and ^{13}C NMR.

A unidirectional process would generate identical conversions of stable to unstable isomer and *cis* to *trans* isomer. This was observed in the experiments described. Crucially, after heating both samples, the ^{13}C NMRs both revealed a ratio of *cis/trans* of 1/1.2, corresponding to exactly the ratio of stable to unstable obtained in the ^{1}H NMR of the mixture in Path A before heating (as expected for a unidirectional process).

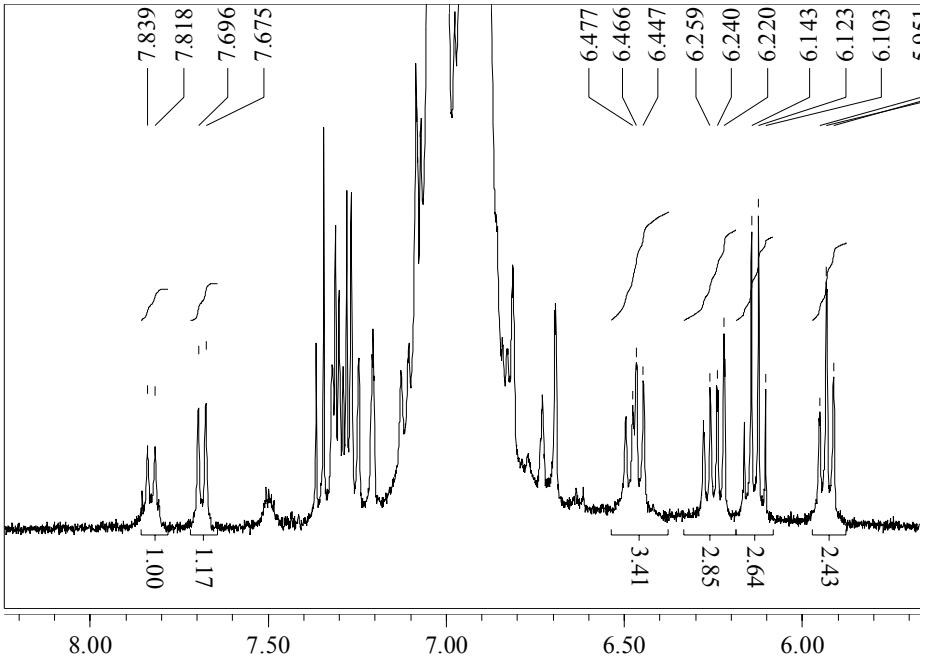

Figure 33: 400 MHz ^{1}H NMR expansion of key signals showing doublet associated with stable form (7.82 ppm) and unstable form (7.68 ppm). The integrals show 1/1.2 stable/unstable ratio.

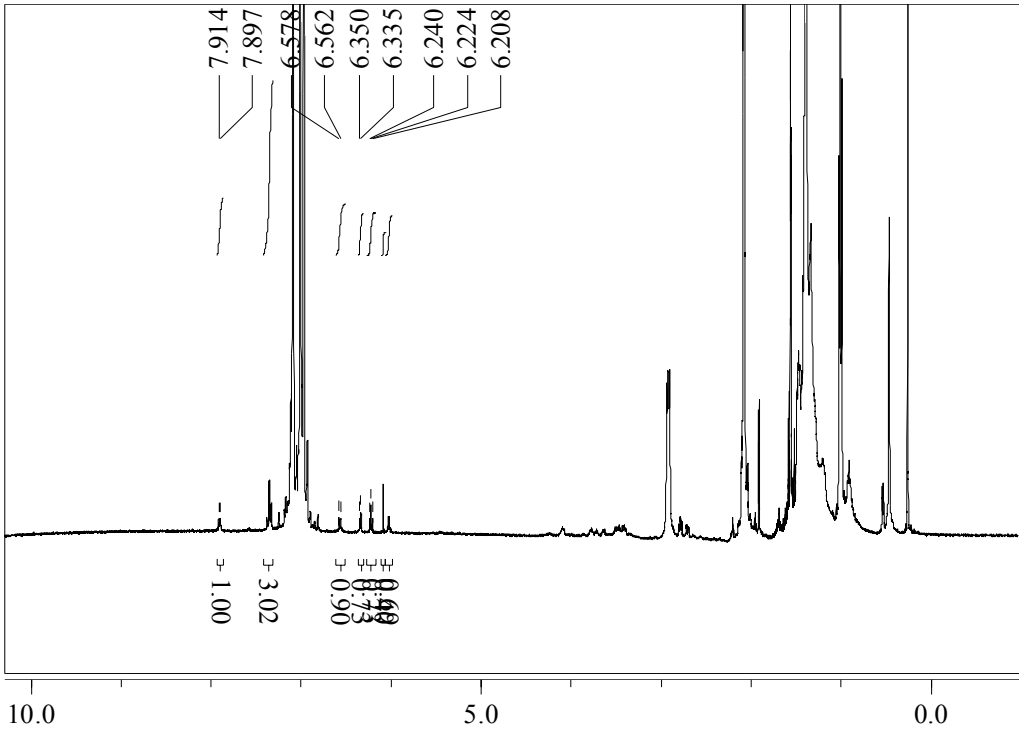

Figure 34: 400 MHz ^{1}H NMR of sample of *cis*-4-Au after irradiation, KCN mediated etching of the gold core, then heating at 70 °C for 2 h.

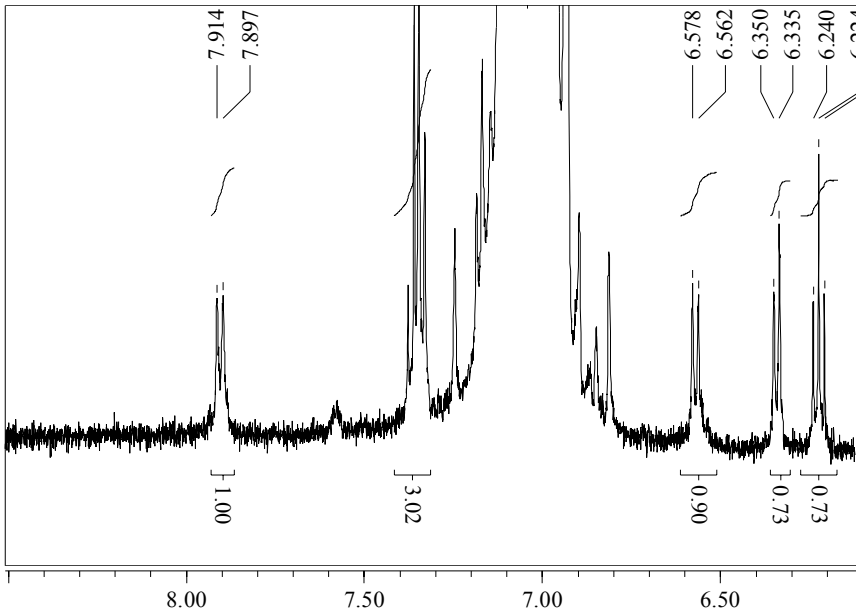

Figure 35: 400 MHz ^{1}H NMR expansion of sample of 4-Au after irradiation, heating at 70 °C for 2 h, then KCN mediated etching of the gold core (end of Path B). This mixture contains a 1.2/1 mixture of stable-*cis*-4 and stable-*trans*-4 (not discernable from the ^{1}H spectrum). Importantly, all unstable isomer is gone as judged by the absence of a peak at 7.68 ppm. This spectrum is essentially identical to the ^{1}H NMR obtained by Path A.

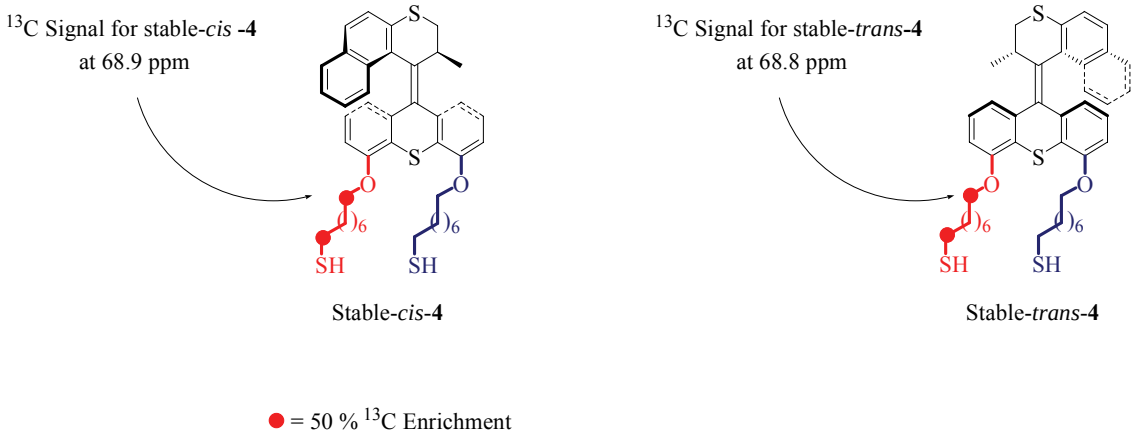

Figure 36: The distinct NMR signal from the ^{13}C labeled ether carbon flanking the motor allowed quantitative detection of *cis* to *trans* isomerisation.

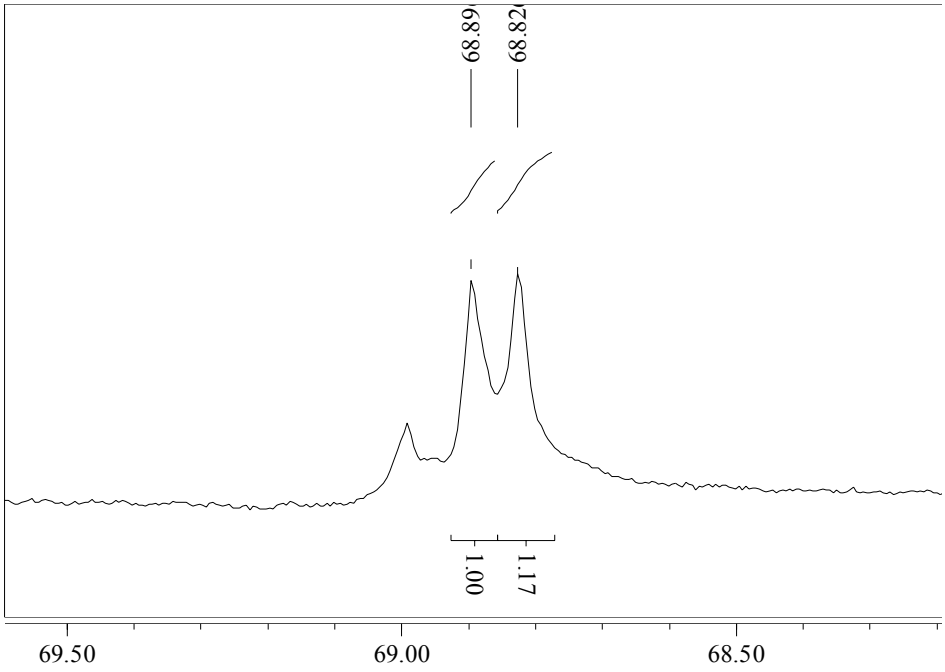

Figure 37: Expansion of 500 MHz ^{13}C NMR of a sample of *cis*-4-Au after irradiation, KCN mediated etching of the gold core, then heating at 70 °C for 2 h (Path A). The new *cis/trans* ratio of 1.0/1.2 is consistent with the amount of unstable isomer generated (1.0/1.2 : stable-4/unstable-4).

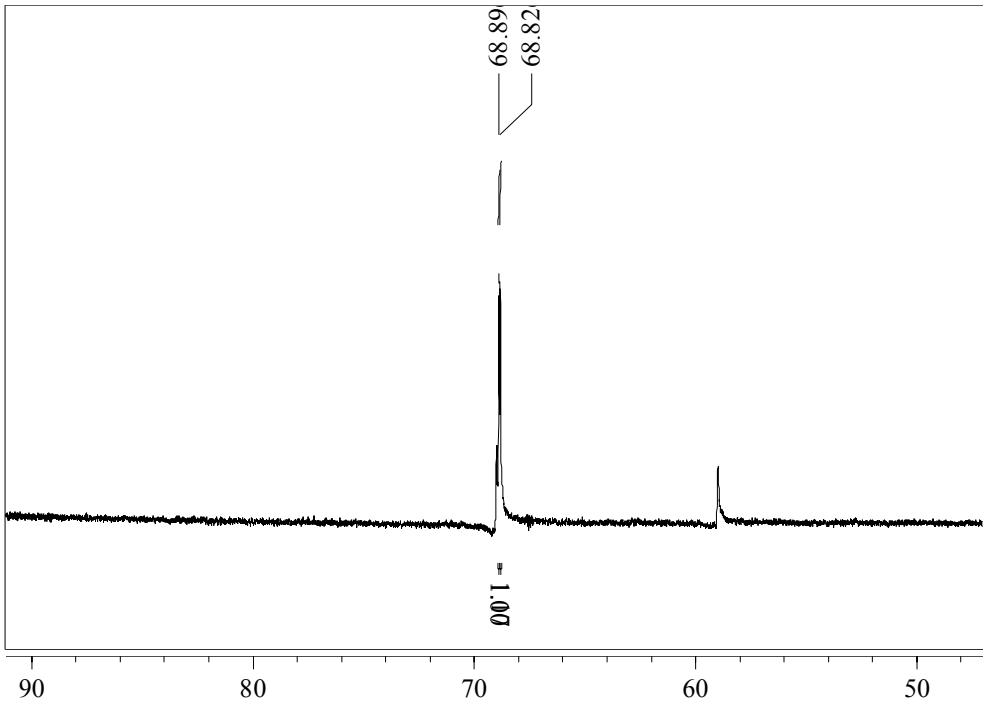

Figure 38: 500 MHz ^{13}C NMR of a sample of *cis*-4-Au after irradiation, KCN mediated etching of the gold core, then heating at 70 °C for 2 h (Path A).

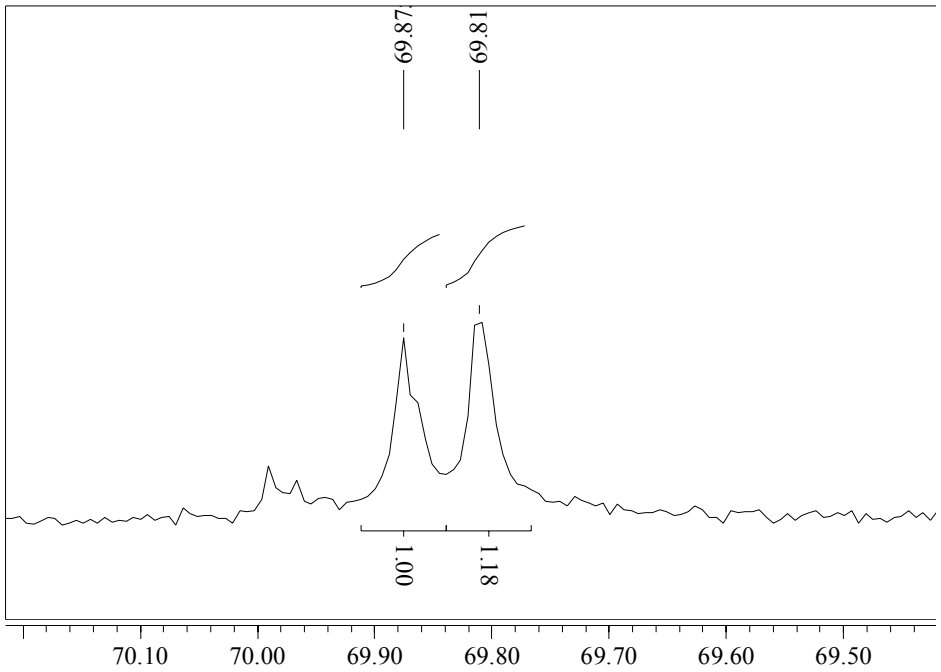

Figure 39: 500 MHz ^{13}C NMR expansion of a sample of *cis*-4-Au after irradiation, heating at 70 °C for 2 h, then KCN mediated etching of the gold core, liberating free motor (Path B). The new *cis/trans* ratio of 1.0/1.2 is consistent with the amount of unstable isomer generated (1.0/1.2: stable-4/unstable-4).

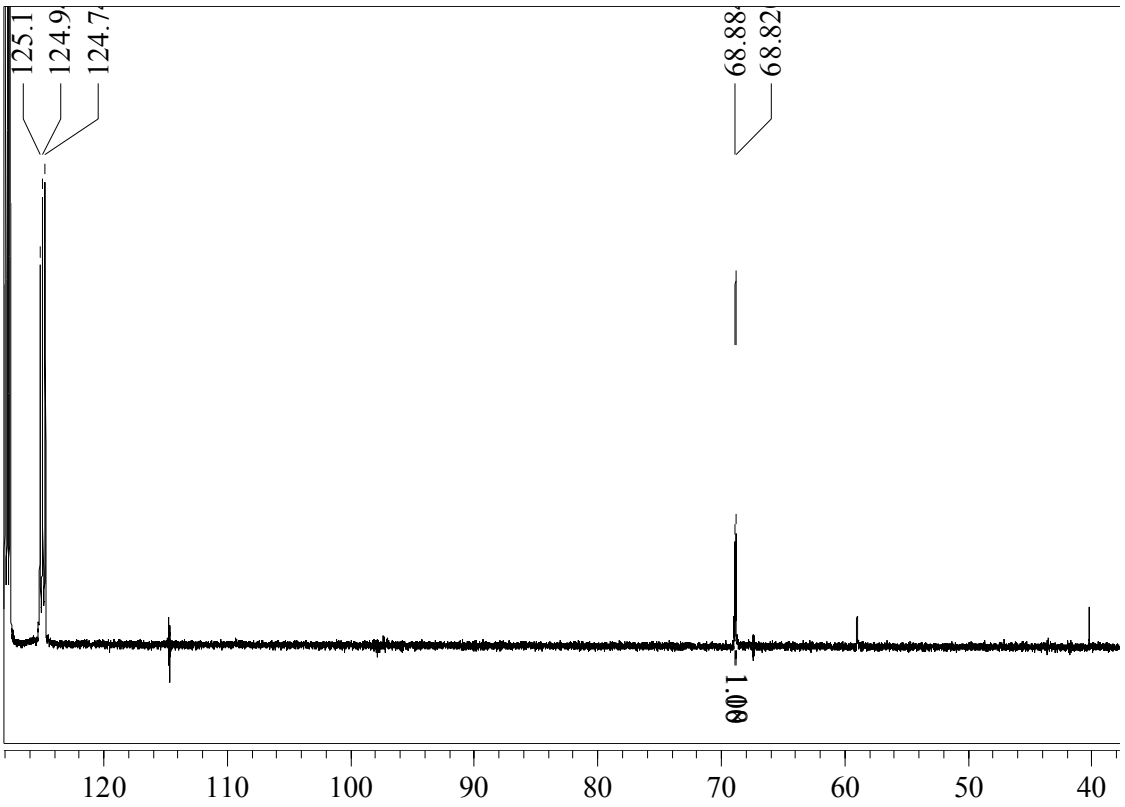

Figure 40: 500 MHz ^{13}C NMR in toluene D_8 of a sample of *cis* 4-Au after irradiation, heating at 70 °C for 2 h, then KCN mediated etching of the gold core, liberating free motor (Path B). See the expansion for integration.

Section 5: General remarks.

The high-resolution ^{1}H NMR spectra were obtained using a Varian VXR-300, Varian Mercury Plus and a Varian Unity Plus Varian-500 operating at 299.97, 399.93 and 499.86 MHz, respectively, for the ^{1}H nucleus. ^{13}C NMR spectra were recorded on a Varian Mercury Plus and a Varian Unity Plus Varian-500 operating at 100.57 and 125.70 MHz, respectively. Chemical shifts are reported in δ units (ppm) relative to the residual deuterated solvent signals of $CHCl_3$ (^{1}H NMR: δ 7.26 ppm; ^{13}C NMR: δ 77.0 ppm) and toluene (^{1}H NMR: δ 2.04 ppm, ^{13}C NMR: δ 20.4 ppm). The splitting patterns are designated as follows: s (singlet), d (doublet), t (triplet), q (quartet), quin (quintet), m

(multiplet) and br (broad). Irradiation experiments were performed with a 180 W Oriel Hg-lamp using a pyrex filter or 365 nm bandwidth filters or a Spectroline ENB-280C/FE UV lamp at 366 nm. UV-Vis measurements were performed on a Hewlett-Packard HP 8453 FT spectrophotometer and CD spectra were recorded on a JASCO J-715 spectropolarimeter using Uvasol grade solvents (Merck). Thermal helix inversions were monitored by CD spectroscopy using the apparatus just described and a JASCO PFD-350S/350L Peltier type FDCD attachment with a temperature control.

---

[1] Chen, S. & Murray, R.W. Arenethiolate monolayer-protected gold clusters. *Langmuir* **15**, 682-689 (1999).

[2] Provencher, S.W. A constrained regularization method for inverting data represented by linear algebraic or integral equations. *Comput. Phys. Commun.* **27**, 229-227 (1982).